

Original Article
Medical Imaging



Computed Tomography-Based Preoperative Simulation System for Pedicle Screw Fixation in Spinal Surgery

Woochan Wi ,^{1*} Sang-Min Park ,^{2*} and Byung-Seok Shin ¹

¹Department of Computer Engineering, Inha University, Incheon, Korea

²Department of Orthopaedic Surgery, Seoul National University Bundang Hospital, Seoul National University College of Medicine, Seongnam, Korea



Received: Dec 1, 2019

Accepted: Mar 1, 2020

Address for Correspondence:

Byeong-Seok Shin, PhD

Department of Computer Engineering, College of Engineering, Inha University, 100 Inha-ro, Michuhol-gu, Incheon 22212, Republic of Korea.
E-mail: bs shin@inha.ac.kr

*Woochan Wi and Sang-Min Park contributed equally to this work.

© 2020 The Korean Academy of Medical Sciences.

This is an Open Access article distributed under the terms of the Creative Commons Attribution Non-Commercial License (<https://creativecommons.org/licenses/by-nc/4.0/>) which permits unrestricted non-commercial use, distribution, and reproduction in any medium, provided the original work is properly cited.

ORCID iDs

Woochan Wi
<https://orcid.org/0000-0001-7759-3762>
Sang-Min Park
<https://orcid.org/0000-0001-6171-3256>
Byung-Seok Shin
<https://orcid.org/0000-0001-7742-4846>

Funding

This work was supported by an Institute for Information & Communications Technology Promotion (IITP) grant funded by the Korean government (MSIT) (No.2017-0-01815, Development of AR-based Surgery Toolkit and Applications)

ABSTRACT

Background: A preoperative planning system facilitates improving surgical outcomes that depend on the experience of the surgeons, thanks to real-time interaction between the system and surgeons. It visualizes intermediate surgical planning results to help surgeons discuss the planning. The purpose of this study was to demonstrate the use of a newly-developed preoperative planning system for surgeons less experienced in pedicle-screw fixation in spinal surgery, especially on patients with anatomical variations.

Methods: The marching cubes algorithm, a typical surface extraction technique, was applied to computed tomography (CT) images of vertebrae to enable three-dimensional (3D) reconstruction of a spinal mesh. Real-time processing of such data is difficult, as the surface mesh extracted from high-resolution CT data is rough, and the size of the mesh is large. To mitigate these factors, Laplacian smoothing was applied, followed by application of a quadric error metric-based mesh simplification to reduce the mesh size for the level-of-detail (LOD) image. Taubin smoothing was applied to smooth out the rough surface. On a multiplanar reconstruction (MPR) cross-sectional image or a 3D model view, the insertion position and orientation of the pedicle screw were manipulated using a mouse. The results after insertion were then visualized in each image.

Results: The system was used for pre-planning pedicle-screw fixation in spinal surgery. Using any pointing device such as a mouse, surgeons can manipulate the position and angle of the screws. The pedicle screws were easy to manipulate intuitively on the MPR images, and the accuracy of screw fixation was confirmed on a trajectory view and 3D images. After surgery, CT scans were performed again, and the CT images were checked to ensure that the screws were inserted properly.

Conclusion: The preoperative planning system allows surgeons and students who are not familiar with pedicle-screw fixation to safely undertake surgery following preoperative planning. It also provides opportunities for screw-fixation training and simulation.

Keywords: Surgical Planning; Pedicle-Screw Fixation; Spinal Surgery; Mesh Smoothing

Disclosure

The authors have no potential conflicts of interest to disclose.

Author Contributions

Conceptualization: Park SM, Wi W, Shin BS.
Data curation: Park SM, Wi W. Formal analysis: Park SM, Wi W. Methodology: Wi W, Shin BS.
Software: Wi W. Validation: Park SM. Writing - original draft: Park SM, Wi W. Writing - review & editing: Shin BS, Park SM.

INTRODUCTION

Pedicle-screw fixation is a common procedure in spinal surgery.^{1,2} Failure to insert the screw correctly may have catastrophic consequences, such as pedicle fracture, nerve injury, and vascular injury, resulting in poor surgical outcomes.³ Anatomical variations of vertebrae make it difficult to insert pedicle screws. Generally, to increase the accuracy of screw fixation, spinal computed tomography (CT) is performed prior to surgery to evaluate surgical anatomy. The CT images are then uploaded to imaging systems, such as a picture archiving and communication system (PACS), and checked by the surgeon to determine the accurate screw position, but typical imaging systems produce only simple tomography images that do not allow the surgeon to plan the exact entry point, convergence angle, length, or diameter of the screws. In addition, it is difficult to reenact the trajectory of the screws, because it is not possible to save the preoperative plan and check the three-dimensional (3D) images during surgery.

Many preoperative planning functions are included in specific spinal navigation systems, but they can be costly and burdensome to use, precluding their use for most surgeons. Although we can use the 3D slicer, the only freely-available software,⁴ it has various limitations and is complicated to use. Further, it is not suitable for pedicle screw-fixation planning. Recent studies have introduced newly-developed software that can be used for simulations of pedicle screw planning, but it is not yet available in Korea.⁵⁻⁸

We have developed a preoperative planning system that allows surgeons to plan the pedicle screw's entry point and convergence angle before spine surgery and to measure its diameter and length to scale. Our simulator provides 3D images and multiplanar reconstruction (MPR) images simultaneously. Thus, it can be used to plan the safe, optimal trajectory for proper placement to avoid nerve root damage. It is easy to reenact the screw path during the actual surgery by referring to the previously planned path. Especially in cases of deformities or anatomic variations, the system can be valuable for preplanning, and it can greatly enhance the safety of surgery performed by less experienced surgeons on patients with complex anatomic variations, such as scoliosis.⁶⁻¹¹

METHODS**Preoperative planning***Real-time interaction under various viewing conditions*

Our system provides a variety of views, such as MPR sectional and trajectory views and a 3D view. The MPR sectional view presents reconstructed images of three mutually perpendicular axes (X, Y, and Z) of the section. The trajectory MPR view presents reconstructed images of the cross-section perpendicular to the fixation direction of the screw and two cross-sections perpendicular to the first. Thus, the anatomical structure in the area of the screw placement can be clearly visualized (Fig. 1). The simulator receives the digital imaging and communications in medicine format image files obtained through CT, which are used to construct an image volume dataset. It resamples the volume to reconstruct MPR and trajectory MPR images. The 3D view shows the three-dimensional model of the spine generated from the 3D reconstruction process and screw models as a cylindrical shape.⁵ The screws are inserted in the model with an "insert" button. Generally, the spinal model is displayed as a translucent model, but it can be changed to opaque as needed.

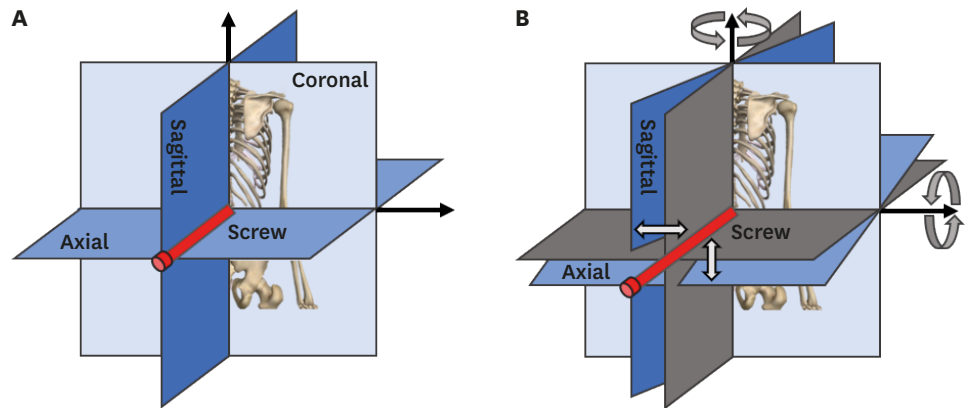


Fig. 1. The constructions of the MPR and its trajectory. (A) MPR sections, (B) trajectory of the MPR sections. MPR = multiplanar reconstruction.

Since all these views are mutually connected, a single user's action on a view is reflected on other views. The input volume data and reconstructed 3D spinal models are defined in the different coordinate systems. Thus, the simulator stores the screw positions in this coordinate system normalized to a value between 0 and 1 to preserve coordinate consistency between the input volume data and the spinal geometric model. The normalized screw position inserted during the planning is recalculated when displayed on each view (Fig. 2).

Users can select and modify the virtual screws on the 3D model view. To do so, one point on the model must be selected. For this, casting a ray in the viewing direction of the mouse click point as the starting point finds the intersection of the triangle. Several triangles appear in this process. Among them, triangles in which the dot product of a normal vector and the ray direction is zero are excluded because they are invisible. The closest triangle is then selected by calculating the distance between the intersection point on the triangle and the starting point of the ray.

Surgical planning on 3D spinal model

With our simulator, the user can make a number of attempts to determine the screw-fixation position before actual spinal surgery without risk to the patient. This also enables predicting the difficulty of the surgery. The real-time interactions between the simulator and users allow multiple surgeons with varying levels of experience to share in visualizing the surgical planning simultaneously. Users can freely change the position and angle of the screws and

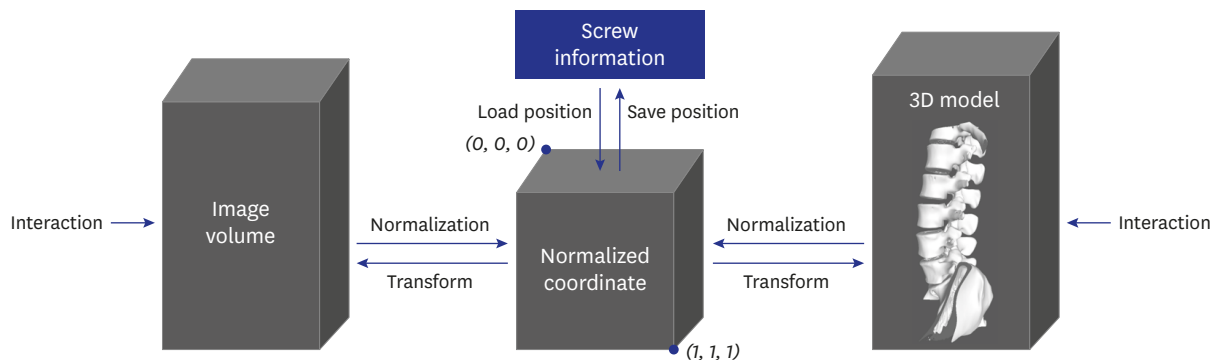


Fig. 2. The flow of preservation of coordinate consistency on the multiplanar reconstruction, trajectory of MPR, and 3D models using the normalized coordinate system. 3D = three-dimensional.

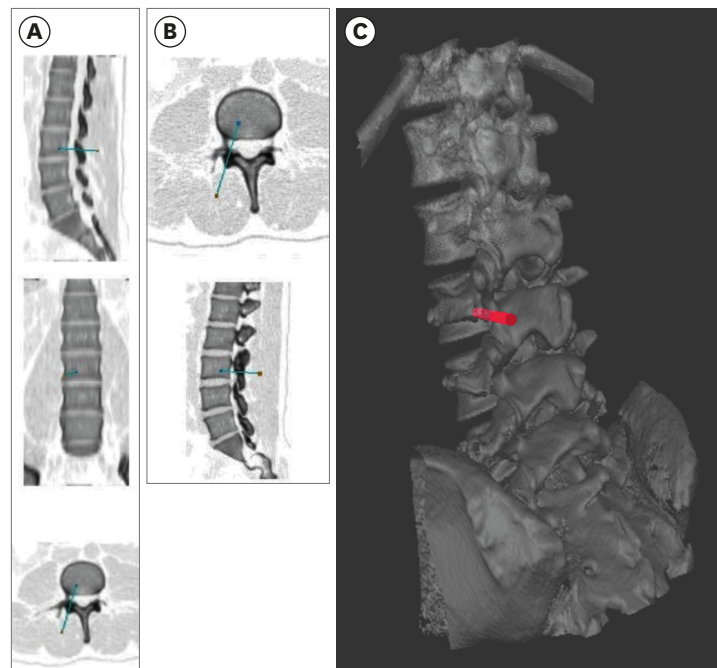


Fig. 3. MPR, trajectory of MPR section views, and 3D-view screenshots on the simulator. (A) MPR section view with a screw inserted, (B) trajectory MPR section view, and (C) 3D model view. Colors of the captured MPR and trajectory MPR view images were reversed to improve visibility. MPR = multiplanar reconstruction, 3D = three-dimensional.

produce MPR section, trajectory MPR section, and 3D model views; users are completely immersed in surgical planning.

The fixation positions of the pedicle screws are determined on the MPR section view, and those are displayed to the MPR, the trajectory MPR, and the 3D views in the simulator. Users can select the screw fixation function and click the mouse on one of the MPR sections to examine the starting and ending point of a screw having a predefined length, diameter, and color, and these parameters are then recorded in the simulator (Fig. 3). The screws are recorded in order in the screw list in the simulator. When users select screws from the list, the corresponding screws are highlighted in a specified color in the MPR view and 3D model view. The length and diameter of the screws can be selected by using the existing inserted screw and modifying the values in a dialogue box (Fig. 4). The degree of angle of the screws can be changed on the 3D model view by dragging one or both of their end points. When changing the angle as above, the simulator updates the starting point of the screw using the direction from the ending point to the starting point and the screw length to keep the length constant (Fig. 5). The length and diameter of the screw can be changed by adjusting the dialog value of the screw selected.⁶

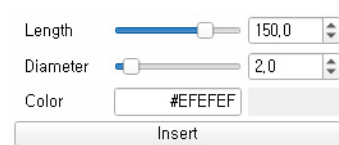


Fig. 4. Screw parameter correction dialog of the simulator providing options to change length, diameter, and color in the simulator.

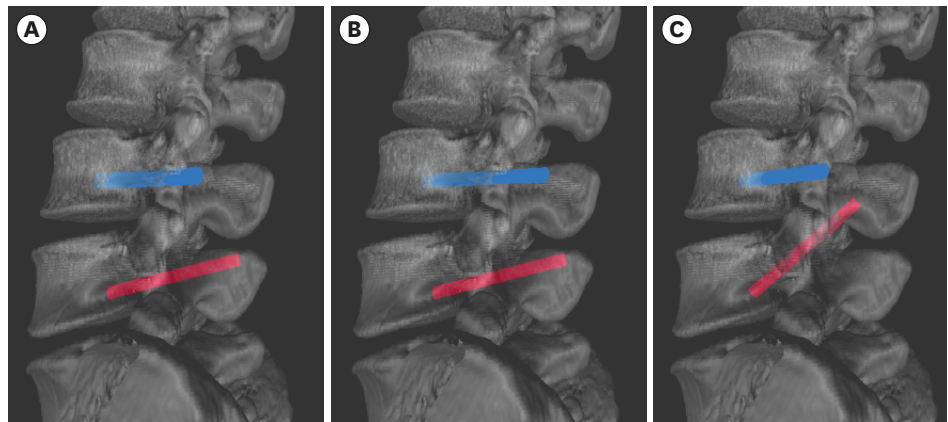


Fig. 5. Comparison of screw models on 3D view with pedicle-screw correction in the simulator. **(A)** Screws with a length of 50 mm and diameter of 5 mm, **(B)** screws with a length of 65 mm and diameter of 4 mm, and **(C)** screws modified to different degrees on the 3D model view. 3D = three-dimensional.

Reconstruction and mesh smoothing of the 3D level-of-detail (LOD) model

The input data are the tomography images scanned by CT devices before spinal surgery. In our system, the marching cubes algorithm was used to reconstruct the 3D mesh.¹² The roughness of the mesh surface, partial volume effects, and noise that occur during CT scanning make it difficult to construct a complete manifold model using the marching cubes algorithm.¹³⁻¹⁵ In addition, overload on rendering pipelines may occur due to multiple vertices, requiring additional simplification or smoothing. We apply Laplacian smoothing¹⁶⁻¹⁸ to smooth the rough surface of the mesh reconstructed by the marching cubes algorithm, and apply a mesh simplification algorithm based on quadric metrics to generate an LOD model after applying Laplacian smoothing, and finally, we apply Taubin smoothing to smooth the 3D model to be displayed in our simulator (Fig. 6).^{19,20}

Using the marching cubes algorithm, an image volume was constructed by stacking multiple images, and eight cubically adjacent neighborhoods of each voxel were then examined to compare with the value of the object boundary desired. A 3D mesh was then reconstructed by referring to the table in which the mesh pattern corresponding to the result of the comparison was defined.^{21,22} This has the advantage of parallel processing by referring to the predefined mesh pattern table.²³

The quadric error metric mesh simplification algorithm was used to calculate the sum Q_p of quadric Q_1 and Q_2 for any vertex pair (v_1, v_2) in the mesh and to calculate the minimum error $EQ_p = \bar{v}^T Q_p \bar{v}$ at the time of decimating the vertex pair to a new vertex, \bar{v} . Decimating the vertex pair with the minimum error was performed repeatedly.^{24,25} This method has a lower error rate and execution time but higher memory usage than other mesh simplification algorithms.²⁶ A low error rate and execution time are more important than low memory usage in preoperative planning, because our system is executed on a workstation or PC.

Laplacian smoothing was applied to smooth out the mesh generated by marching cubes.^{16,18} Laplacian smoothing can cause mesh shrinkage. The mesh shrinkage rate of Laplacian smoothing increases as mesh density decreases or as the number of iterations increases.^{27,28} Mesh shrinkage resulting from smoothing algorithms precludes the ability to preserve the whole shape and the spinal canal shape of the spinal mesh, meaning that surgeons cannot

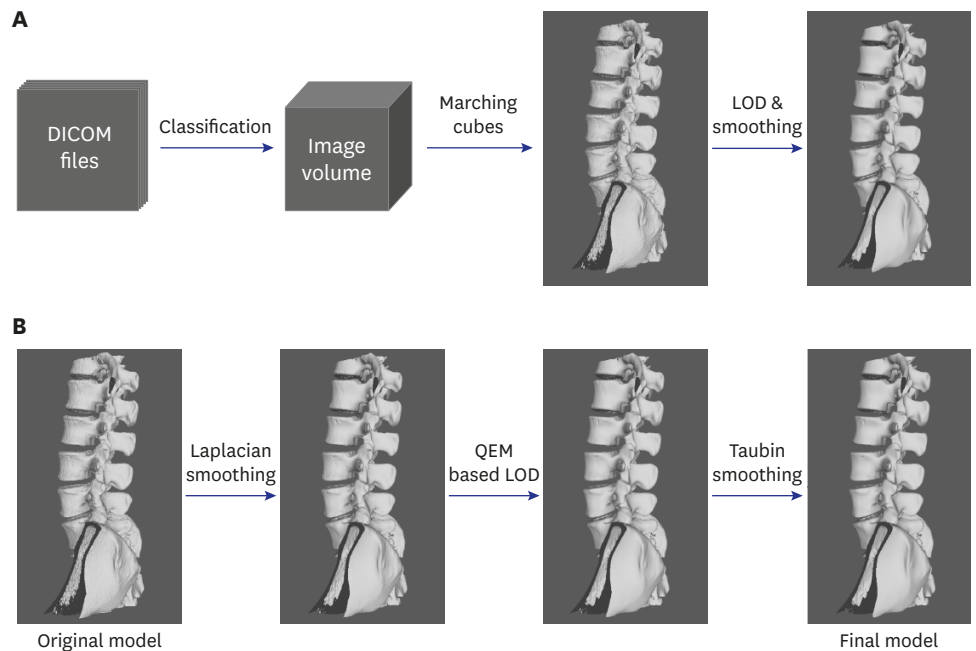


Fig. 6. 3D model reconstruction and additional process in this study. **(A)** Overall process of 3D model reconstruction using DICOM format computed tomography images, **(B)** additional smoothing and LOD application process for the original model created using the marching cube algorithm. DICOM = digital imaging and communications in medicine, LOD = level-of-detail, QEM = quadric error metric, 3D = three-dimensional.

plan surgery precisely. For these reasons, we applied Laplacian smoothing before generating the LOD models of the spinal mesh and only a small number of iterations.

Laplacian smoothing was applied to move a vertex, v_i in the mesh to a new vertex, v_{new} . v_{new} is the weighted average for N-adjusted vertices, v_j . The equation to obtain v_{new} can be expressed as:

$$v_{new} = v_i + \lambda L(v_i),$$

where $L(v_i)$ is a vector average between the vertex v_i and the adjusted vertices v_j . $L(v_i)$ can be expressed as follows:

$$L(v_i) = \frac{1}{\sum_{j=1}^N w_{ij}} \left(\sum_{j=1}^N w_{ij} v_j \right) - v_i.$$

When w_{ij} was the weight of each of the adjusted vertices, the cotangent weight was used, as follows:

$$w_{ij} = \frac{1}{2} (\cot \alpha_{ij} + \cot \beta_{ij}).$$

Although Laplacian smoothing was applied before generating the LOD models, the surface of the mesh generated by the LOD algorithms may not be smooth. Therefore, additional smoothing was required to smooth the surface after generating the LOD models. As the LOD model has a low vertex density, repeated applications of Laplacian smoothing may result in greater mesh shrinkage than when the vertex density is low. Therefore, Taubin smoothing

was applied instead of Laplacian smoothing.^{29,30} Although it has less smoothing effect than Laplacian smoothing, it can prevent mesh shrinkage via the application of a mesh shrinkage step and an expansion step in each iteration.^{29,31} Each step of Taubin smoothing is similar to Laplacian smoothing. These two steps can be expressed as:

$$\text{Step 1: } v'_i = v_i + \lambda L(v_i), \lambda > 0.$$

$$\text{Step 2: } v_{new} = v'_i + \mu L(v'_i), \mu < 0.$$

where the parameters λ and μ are the scale variables of $L(v_i)$, and the weight of $L(v_i)$ in Taubin smoothing can be chosen in a variety of ways. We applied the same weight as in Laplacian smoothing.³² Thus, in the first step of Taubin smoothing, the mesh shrinks as in Laplacian smoothing. In the second step, the mesh expands by reversing the sign of the scale variable. These two smoothing steps produced the smoothing effect and prevented mesh shrinkage.

Application

Patient population and radiographic evaluation

We retrospectively reviewed postoperative CT data of 16 patients who underwent pedicle screw fixation in the lumbar spine, after preplanning using this preoperative system. The procedures were performed by a single orthopedic surgeon at our tertiary teaching hospital, in September and October 2019.

Planning process

We used the developed simulator in preoperative planning to determine the most appropriate position of pedicle screws in spinal surgery. The appropriate position of pedicle screws is at an angle parallel to the vertebral endplates, with the length and diameter of the pedicle screw passing through the pedicle without damaging the anterior cortex of the vertebral body (Fig. 7). Preoperative planning was carried out for all pedicles that were to have pedicle screws inserted. The screw-fixation planning was mainly carried out on the MPR section, and the trajectory MPR view was used to confirm that each screw was in the proper position (Fig. 8). Finally, we checked the entry point, convergence angle, diameter, and length of the pedicle screws in the 3D image.

The 3D image and trajectory MPR view were used to facilitate screw positioning during the actual operations. Postoperative CT scans were reviewed to ensure that the screws were properly inserted in comparison with preoperative pedicle-screw planning (Figs. 9 and 10).

Radiographic evaluation

The accuracy of pedicle-screw placement was evaluated using postoperative CT by two independent orthopedic surgeons (OK, a fourth-year orthopedic resident, and HH, a third-year orthopedic resident). The accuracy of pedicle-screw position was measured using Gertzbein and Robbins classification: Grade A, the screw is completely within the pedicle; Grade B, the screw breaches the pedicle's cortex by less than 2 mm; Grade C, pedicle cortical breach is between 2 and 4 mm; Grade D, pedicle cortical breach is between 4 and 6 mm; and Grade E, pedicle cortical breach is 6 mm or more.³³

Statistical analysis

Interobserver agreement was analyzed using kappa values. The level of agreement was interpreted as slight when kappa value was 0 to 0.2, fair when kappa value was 0.2 to 0.4,

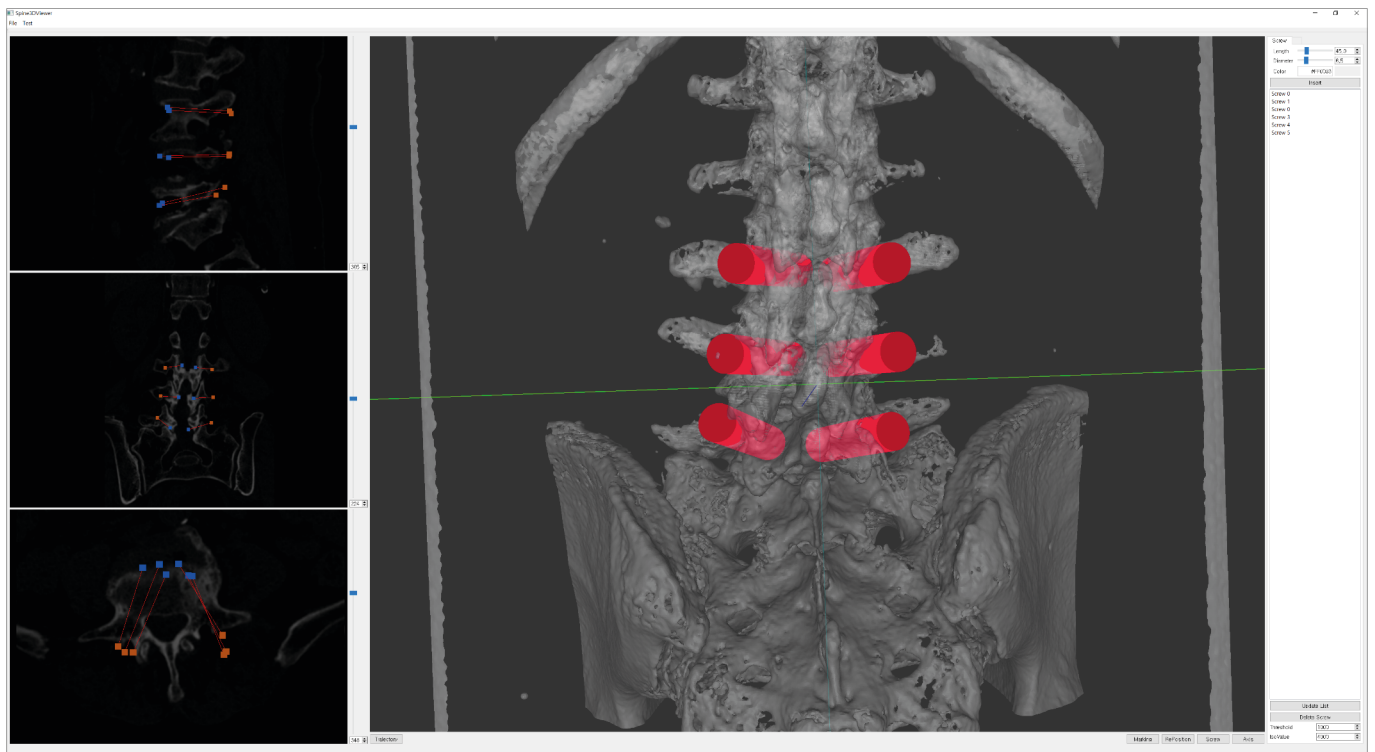


Fig. 7. A screenshot of screw-fixation planning on the multiplanar reconstruction section view.

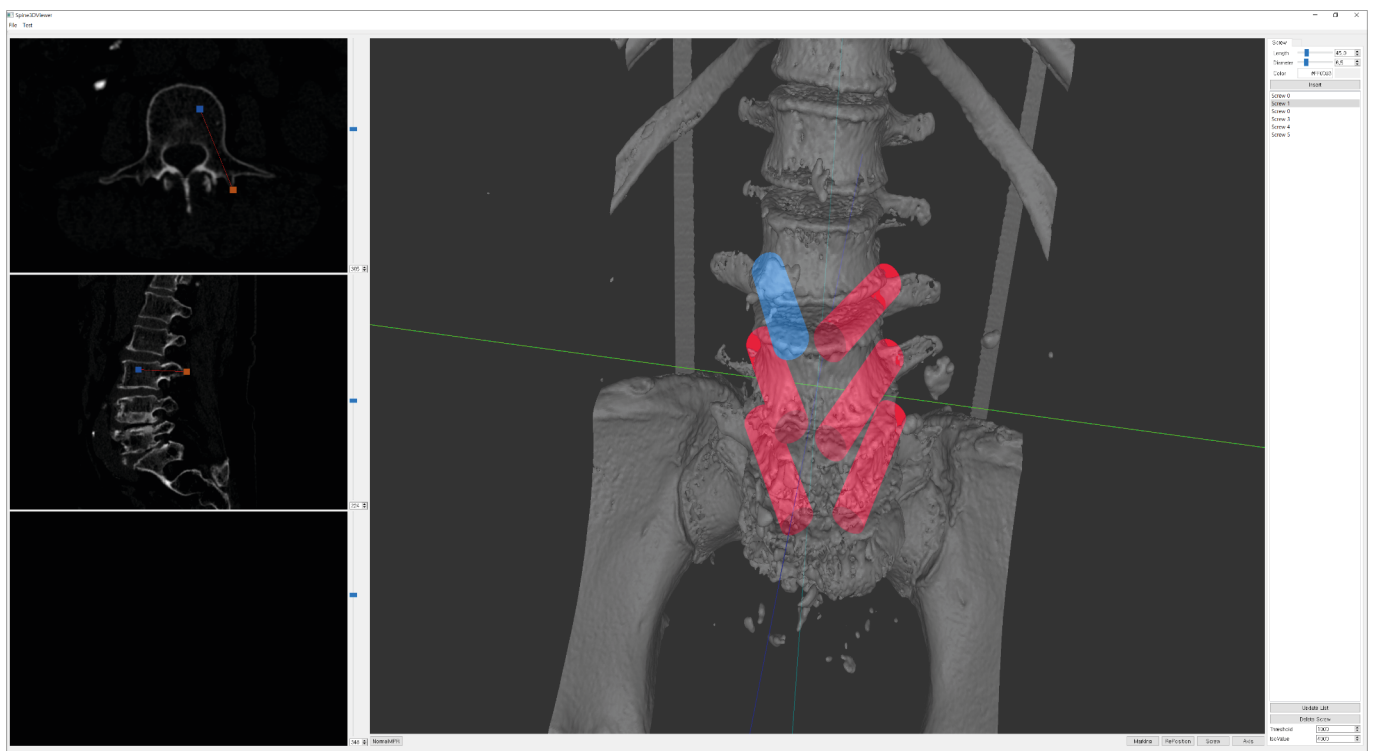


Fig. 8. Correction of the pedicle-screw angle using the three-dimensional model view and the fixation position on the trajectory multiplanar reconstruction section view.



Fig. 9. Results of pedicle-screw fixation using external software.

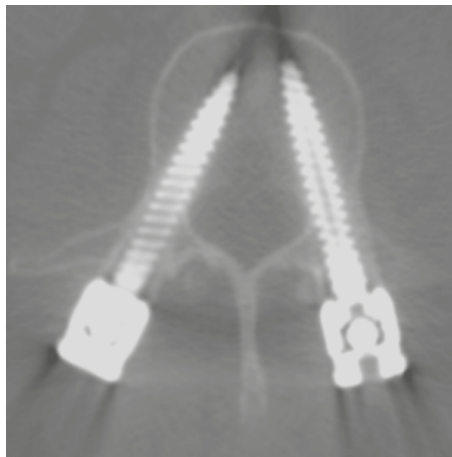


Fig. 10. Computed tomography images taken to confirm the results after screw-fixation surgery.

moderate when kappa was 0.4 to 0.6, substantial when kappa value was 0.6 to 0.8, and almost perfect when kappa value was greater than 0.8. Stata/MP 15.0 (Stata Statistical Software, Release 15; StataCorp LLC, College Station, TX, USA) was used for the statistical analysis.

Ethics statement

This retrospective case series study of pedicle screw placement after the use of the preoperative pedicle screw planning system was approved by the Institutional Review Boards of Seoul National University Bundang Hospital, who waived informed consent (B-1911-576-101).

RESULTS

The 16 patients included in our study consisted of 6 (38%) men and 10 (62%) women, with a mean age of 67.9 years (range, 54–83 years) at the time of first visit. A total of 82 pedicle screws were reviewed in our study. Detailed demographic data are shown in **Table 1**.

Table 1. Demographic data of the patients included in this study

Characteristics	Values
No. of patients	16
Mean age, yr	68.0 (54–83)
Gender, men/women	7/9
Mean height, cm	158.1 (147.5–173.5)
Mean weight, kg	65.7 (51.6–89.6)
Body mass index, kg/m ²	26.3 (22.1–37.4)
Screw placed level	
L1	0
L2	2
L3	14
L4	30
L5	28
S1	8

Data are presented as mean (range) or number (%).

Table 2. The accuracy grade of pedicle-screw placement

Grade of pedicle screw placement	Screw
A	66 (80.5)
B	13 (15.9)
C	2 (2.4)
D	0 (0)
E	1 (1.2)
Total	82 (100)

Data are presented as number (%).

The rate of grade A accuracy of pedicle-screw fixation was 80.5%, and the rate of grade A and grade B accuracy combined was 96.4%. The failure rate of pedicle-screw fixation was 3.6% (**Table 2**). There were no cases of neurovascular injury or life-threatening major complications. There was almost perfect agreement between observers for evaluating pedicle-screw accuracy by CT (kappa value = 0.896).

An LOD model was generated and compared to each model according to smoothing algorithms applied (**Fig. 11**). The LOD model reduced vertices of the mesh generated by marching cubes to about 10%. The model has 265,525 vertices. Laplacian smoothing was applied in 8 iterations and Taubin smoothing was applied in 30 iterations. One of the Taubin smoothing parameters, λ , is 0.50, and the other, μ , is -0.53 .

The model was compared visually and measured for errors according to the smoothing algorithm type and iterations before and after the LOD model was generated (**Fig. 12** and **Table 3**). The average Hausdorff distance was applied to assess the error.^{34,35} Five hundred thousand sample points were taken from the LOD model without any smoothing, and this was used to measure the error with the model after smoothing.

Table 3. The Hausdorff distance by number of smoothing applications

Taubin smoothing iterations	Laplacian smoothing iterations		
	4	12	20
10	0.15	0.22	0.28
30	0.18	0.24	0.29
50	0.20	0.25	0.29

Errors are rounded to nearest one-hundredth (two decimal places).

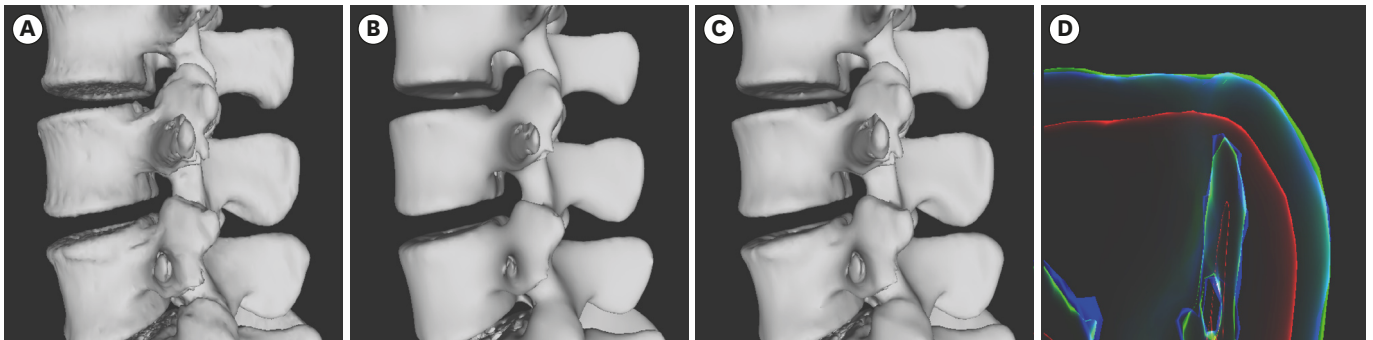


Fig. 11. Visual comparison of LOD model and models of application of Laplacian and Taubin smoothing. (A) The LOD model, (B) the model that applied Laplacian smoothing in 8 iterations, (C) the model that applied Taubin smoothing in 30 iterations, (D) rendering image using x-ray shader for visual comparison of these models. The blue outline is the outline of (A), the red is (B) and the green is (C). LOD = level-of-detail.

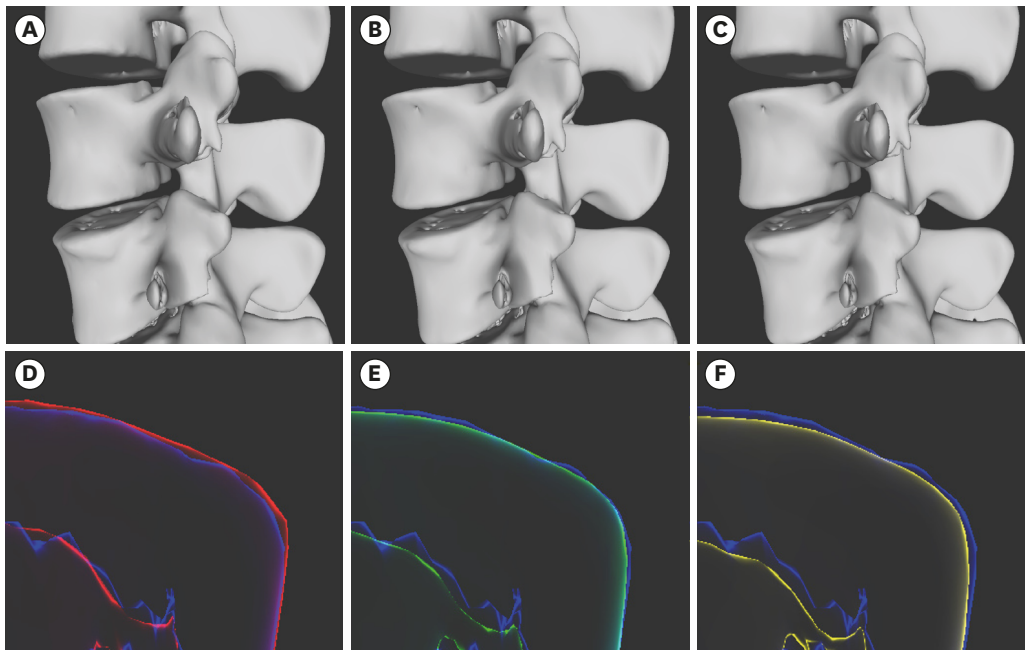


Fig. 12. Visual comparison of results models according to the number of Laplacian and Taubin smoothing applications. (A), (B), and (C) are the models that received 4, 12, and 20 iterations of Laplacian smoothing and 50, 30, and 10 iterations of Taubin smoothing. (D), (E), and (F) are the rendering images using X-ray shader for visually comparing the model size changes according to the iterations of each smoothing algorithm applied. The blue outline is the level-of-detail model, as in Fig. 11A.

DISCUSSION

Pedicle-screw fixation is a common procedure in spinal surgery. It is technically difficult, requiring a prolonged learning period. Pedicle screw-related complications occur, especially early in the learning period. Our preoperative planning system is useful for accurate pedicle-screw planning of entry point, convergence angle, length and diameter, and 3D visualization of planned pedicle screws.

Eftekhar et al.⁹ developed a program in Windows to simulate pedicle-screw fixation on the vertebral body, but the program was impractical because it could not analyze patients' specific anatomical variations. Klein et al.¹¹ developed software in the form of a plug-in for

AmiraDev software (Visage Imaging, Carlsbad, CA, USA). Similar to our software, it has the advantage of preoperative planning for each patient by CT, but AmiraDev is inconvenient for use in the clinical setting because it is commercial software with a prohibitive cost. In a recent study, the authors introduced a pedicle screw simulator for use before actual operations,⁶ but it can be used only experimentally, as it has not been used in real-world conditions.

There is commercial spinal planning software from Brainlab (Brainlab, Munich, Bayern, Germany), but it is designed for planning during surgery and part of a system configured for use with other surgical equipment. While it provides MPR and trajectory views, it lacks a 3D view. Surgimap is free software for surgical planning (Nemaris, NY, USA), but it does not provide a 3D view and allows surgical planning for a single image only. The length and diameter of pedicle screws can be determined and corrected on the image using only a mouse, but it cannot correct directly by changing numerical values. The 3D Slicer is open-source image analysis and visualization software freely available. The spinal surgery planning feature is provided in a downloadable extension of the program called the Pedicle Screw Simulator. This extension works well for our purposes, but the pedicle screw in the extension cannot be inserted and corrected using mainly the view, but only in the dialog screen, making it more complicated, and the length and diameter of the insertable screw are limited to certain kinds. In the latest version currently available for download, the available pedicle screws include only 47.5, 55.0, 62.5, and 70.0 mm in length, and 3.0, 3.5, 4.5, and 5.0 mm in diameter.

The software described in the present study allows users to determine the entry point, direction, convergence angle, diameter, and length of pedicle screws before spinal surgery. As in a general PACS, the user first determines the positions of the screws on the MPR view and then affirms these on the 3D model view and trajectory MPR view to ensure that they are planned in the correct positions.

During an actual operation, preplanning makes it easy to see where to insert the screws and at what position and convergence angle (**Fig. 8**). The preoperative planning images can be compared with postoperative CT images to confirm that the screws are similar to the preoperative plan (**Fig. 9**). Our surgical planning system aids preoperative planning by surgeons who are unfamiliar with pedicle-screw fixation and provides them a risk-free environment. It can serve as an aid to training by allowing users to indirectly experience and practice screw fixation in a variety of patients. According to a previously published paper, an accuracy of grade B and higher during pedicle-screw fixation was 92.9%.¹ The accuracy shown in this study is higher than in the previous study, so it can be concluded that preoperative planning is effective in increasing accuracy.

In our system, postprocessing algorithms, such as generating the LOD model and mesh smoothing, are applied to improve the program's execution time and the quality of the model. In particular, we compared the difference of mesh size and the Hausdorff error of the smoothing protocols of Laplacian and Taubin. The outline of the model smoothed by Laplacian smoothing is inside than the LOD model, while the outline of the model smoothed by Taubin smoothing is similar to the LOD model. It can be seen visually that applying Laplacian smoothing to the LOD model can cause unintentional volume shrinkage and shape deformation (**Fig. 11**). Thus, applying Taubin smoothing to the LOD model demonstrated less size shrinkage than Laplacian smoothing.

When Laplacian smoothing was applied before LOD generation and turbine smoothing after, the models were compared visually according to the number of smoothing applications, and no significant difference was found (**Fig. 12**). Numerical error was measured to compare the LOD model and smoothing models. If the number of Laplacian smoothing iterations before generating the LOD model is lower—even if the number of Taubin smoothing iterations is higher—the numerical error is small (**Table 3**). Therefore, it is important to determine accurately the number of iterations of smoothing algorithms that can minimize errors and preserve the mesh size.

In the future, the preoperative planning system will be combined with virtual reality via a virtual simulator of an actual operation to allow users to experience surgery before an actual operation. It could be developed as a planning simulator that can also simulate a real surgical environment. The potential training value of a preoperative planning system for junior surgeons and medical students will first need to be evaluated.

The preoperative planning system is expected to play an increasingly important role in creating a risk-free virtual surgical environment. In particular, it can allow junior surgeons and medical students to practice preoperative planning and perform a simulation. Although the simulator needs further development, we believe that it can play an important role in spinal surgery by increasing familiarity with anatomic deformities, improving surgical outcomes, and reducing complications.

REFERENCES

1. Park SM, Shen F, Kim HJ, Kim H, Chang BS, Lee CK, et al. How many screws are necessary to be considered an experienced surgeon for freehand placement of thoracolumbar pedicle screws?: analysis using the cumulative summation test for learning curve. *World Neurosurg* 2018;118:e550-6.
[PUBMED](#) | [CROSSREF](#)
2. Perna F, Borghi R, Pilla F, Stefanini N, Mazzotti A, Chehrassan M. Pedicle screw insertion techniques: an update and review of the literature. *Musculoskelet Surg* 2016;100(3):165-9.
[PUBMED](#) | [CROSSREF](#)
3. Esses SI, Sachs BL, Dreyzin V. Complications associated with the technique of pedicle screw fixation. A selected survey of ABS members. *Spine* 1993;18(15):2231-8.
[PUBMED](#) | [CROSSREF](#)
4. 3D Slicer. <https://www.slicer.org>. Accessed Date.
5. Song G, Bai H, Zhao Y, Han J, Liu X. Preoperative planning and simulation for pedicle screw insertion using computed tomography-based patient specific volume rendering combined with projection fluoroscopy. *Int Robot Autom J* 2017;2(1):25-9.
[CROSSREF](#)
6. Xiang L, Zhou Y, Wang H, Zhang H, Song G, Zhao Y, et al. Significance of preoperative planning simulator for junior surgeons' training of pedicle screw insertion. *J Spinal Disord Tech* 2015;28(1):E25-9.
[PUBMED](#) | [CROSSREF](#)
7. Yeom JS, Choy WS, Kim WJ, Kim HY, Kang JW, Kim YW, et al. A patient-specific surgical simulation system for spinal screw insertion composed of virtual roentgenogram, virtual C-arm, and rapid prototyping. *J Korean Orthop Assoc* 2001;36(2):161-6.
[CROSSREF](#)
8. Park SK, Yeom JS, Won JH, Lee JC, Lee DH, Lee J, et al. C1-2 fixation using polyaxial screws and rods assisted by computer simulation for revision of failed posterior fusion: a technical report. *J Korean Orthop Assoc* 2005;40(6):778-81.
[CROSSREF](#)
9. Eftekhari B, Ghodsi M, Ketabchi E, Rasaei S. Surgical simulation software for insertion of pedicle screws. *Neurosurgery* 2002;50(1):222-3.
[PUBMED](#)

10. Muralidharan V, Swaminathan G, Devadhas D, Joseph BV. Patient-specific interactive software module for virtual preoperative planning and visualization of pedicle screw entry point and trajectories in spine surgery. *Neurol India* 2018;66(6):1766-70.
[PUBMED](#) | [CROSSREF](#)
11. Klein S, Whyne CM, Rush R, Ginsberg HJ. CT-based patient-specific simulation software for pedicle screw insertion. *J Spinal Disord Tech* 2009;22(7):502-6.
[PUBMED](#) | [CROSSREF](#)
12. Rajon DA, Bolch WE. Marching cube algorithm: review and trilinear interpolation adaptation for image-based dosimetric models. *Comput Med Imaging Graph* 2003;27(5):411-35.
[PUBMED](#) | [CROSSREF](#)
13. Raj Ségonne F, Fischl B. Integration of topological constraints in medical image segmentation. In: Paragios N, Duncan J, Ayache N, editors. *Handbook of Biomedical Imaging*. Boston, MA: Springer; 2015, 245-62.
14. Wang J, Yu Z. Feature-sensitive tetrahedral mesh generation with guaranteed quality. *Comput Aided Des* 2012;44(5):400-12.
[PUBMED](#) | [CROSSREF](#)
15. Zhang Y, Hughes TJ, Bajaj CL. An automatic 3D mesh generation method for domains with multiple materials. *Comput Methods Appl Mech Eng* 2010;199(5-8):405-15.
[PUBMED](#) | [CROSSREF](#)
16. Vollmer J, Mencl R, Müller H. Improved laplacian smoothing of noisy surface meshes. *Comput Graph Forum* 1999;18(3):131-8.
[CROSSREF](#)
17. Manmadhachary A, Ravi Kumar Y, Krishnanand L. Improve the accuracy, surface smoothing and material adaption in STL file for RP medical models. *J Manuf Process* 2016;21:46-5.
[CROSSREF](#)
18. Chartrand G, Cresson T, Chav R, Gotra A, Tang A, De Guise JA. Liver segmentation on CT and MR using Laplacian mesh optimization. *IEEE Trans Biomed Eng* 2017;64(9):2110-21.
[PUBMED](#) | [CROSSREF](#)
19. Wang LC, Hung YC. Hole filling of triangular mesh segments using systematic grey prediction. *Comput Aided Des* 2012;44(12):1182-9.
[CROSSREF](#)
20. Sazonov I, Nithiarasu P. Semi-automatic surface and volume mesh generation for subject-specific biomedical geometries. *Int J Numer Methods Biomed Eng* 2012;28(1):133-57.
[PUBMED](#) | [CROSSREF](#)
21. Jermyn M, Ghadyani H, Mastanduno MA, Turner W, Davis SC, Dehghani H, et al. Fast segmentation and high-quality three-dimensional volume mesh creation from medical images for diffuse optical tomography. *J Biomed Opt* 2013;18(8):86007.
[PUBMED](#) | [CROSSREF](#)
22. Kalaiselvi T, Sriramakrishnan P, Somasundaram K. Survey of using GPU CUDA programming model in medical image analysis. *Inform Med Unlocked* 2017;9:133-44.
[CROSSREF](#)
23. Zhou K, Gong M, Huang X, Guo B. Data-parallel octrees for surface reconstruction. *IEEE Trans Vis Comput Graph* 2011;17(5):669-81.
[PUBMED](#) | [CROSSREF](#)
24. Garland M, Zhou Y. Quadric-based simplification in any dimension. *ACM Trans Graph* 2005;24(2):209-39.
[CROSSREF](#)
25. Papageorgiou A, Platis N. Triangular mesh simplification on the GPU. *Vis Comput* 2015;31(2):235-44.
[CROSSREF](#)
26. Matias van Kaick O, Pedrini H. A comparative evaluation of metrics for fast mesh simplification. *Comput Graph Forum* 2006;25(2):197-210.
[CROSSREF](#)
27. Rypl D, Nerad J. Volume preserving smoothing of triangular isotropic three-dimensional surface meshes. *Adv Eng Softw* 2016;101:3-26.
[CROSSREF](#)
28. Bian Z, Tong R. Feature-preserving mesh denoising based on vertices classification. *Comput Aided Geom Des* 2011;28(1):50-64.
[CROSSREF](#)
29. Petitjean S. A survey of methods for recovering quadrics in triangle meshes. *ACM Comput Surv* 2002;34(2):211-62.
[CROSSREF](#)

30. Gosselin MC, Neufeld E, Moser H, Huber E, Farcito S, Gerber L, et al. Development of a new generation of high-resolution anatomical models for medical device evaluation: the Virtual Population 3.0. *Phys Med Biol* 2014;59(18):5287-303.
[PUBMED](#) | [CROSSREF](#)
31. Deese K, Geilen M, Rieg R. A two-step smoothing algorithm for an automated product development process. *Int J Simul Model* 2018;17(2):308-17.
[CROSSREF](#)
32. Chen CY, Cheng KY. A sharpness dependent filter for mesh smoothing. *Comput Aided Geom Des* 2005;22(5):76-391.
[CROSSREF](#)
33. Gertzbein SD, Robbins SE. Accuracy of pedicular screw placement in vivo. *Spine* 1990;15(1):11-4.
[PUBMED](#) | [CROSSREF](#)
34. Tang M, Lee M, Kim YJ. Interactive Hausdorff distance computation for general polygonal models. *ACM Trans Graph* 2009;28(3):74.
[CROSSREF](#)
35. Bonaretti S, Seiler C, Boichon C, Reyes M, Büchler P. Image-based vs. mesh-based statistical appearance models of the human femur: implications for finite element simulations. *Med Eng Phys* 2014;36(12):1626-35.
[PUBMED](#) | [CROSSREF](#)